

# Two-dimensional non-Hermitian topological phases induced by asymmetric hopping in a one-dimensional superlattice

Junpeng Hou,<sup>1</sup> Ya-Jie Wu,<sup>1,2</sup> and Chuanwei Zhang<sup>1,\*</sup>

<sup>1</sup>*Department of Physics, The University of Texas at Dallas, Richardson, Texas 75080-3021, USA*

<sup>2</sup>*School of Science, Xi'an Technological University, Xi'an 710032, China*

Non-Hermitian systems can host novel topological states with novel topological invariants and bulk-edge correspondences that are distinct from conventional Hermitian systems. Here we show that two unique classes of non-Hermitian 2D topological phases, a  $2\mathbb{Z}$  non-Hermitian Chern insulator and a  $\mathbb{Z}_2$  topological semimetal, can be achieved by tuning staggered asymmetric hopping strengths in a 1D superlattice. These two non-Hermitian topological phases support edge modes with real energy due to robust  $\mathcal{PT}$ -symmetric phase and can coexist in proper parameter regions. The proposed scheme can be experimentally realized in photonic/atomic systems and opens the avenue for exploring novel classes of non-Hermitian topological phases with 1D superlattices.

**Introduction.** In the past few decades, topological states of matter have been extensively studied in various physical systems because of their unusual properties with significant applications in quantum devices and information processing [1, 2]. The study has been mainly focused on electrons in solid-state materials [3], while ultra-cold atomic systems provide another platform for realizing topological states with high tunability and controllability [4–11]. In recent years, the concept of topology has also been generalized to classic systems govern by certain types of wave equations such as optics/phonics [12–18], acoustics [19, 20], and electric circuits [21], yielding many interesting topological states.

One significant feature of these classical systems over quantum materials lies on their capability of controllably inducing non-Hermiticity such as gain and loss, which make them excellent platforms for exploring novel non-Hermitian physics. Interesting physical phenomena induced by non-Hermiticity have been found, including unidirectional transportation [22], spontaneous  $\mathcal{PT}$  symmetry breaking with exceptional points [23, 24], fast eigenstate transition [25] and novel superfluidity [26, 27], etc. In particular, many extraordinary effects and applications have been proposed or demonstrated for non-Hermitian photonics [28–33].

In this context, the combination of the concepts of topological states and non-Hermiticity leads to the emergence of novel topological effects, for instance,  $4\pi$  periodicity, anomalous edge states, non-Bloch wave, non-Hermitian skin effect, etc [34–42]. In experiments, photonic [43–51] and atomic [52, 53] systems naturally provide platforms to realize non-Hermitian topological states. Although in most of these work the non-trivial topology is attributed to the Hermitian part of the Hamiltonian, it has been recently proposed that topological states may be solely induced by non-Hermiticity [47] with a focus on high-order topological insulators [51, 53, 54]. The classification of these non-Hermitian topological phases has been proposed through a reduction from AZ classes [55], but such a classification re-

mains incomplete because a random non-Hermitian matrix belongs to a broader BL class [56].

In Hermitian systems, it is known that 2D topological phases, such as a Chern insulator, can be simulated using a 1D lattice with staggered hopping or on-site potential [57] described by an additional periodic parameter. The experimental realization of such parameter space 2D topological phases could be significantly simpler comparing to their 2D lattice counterparts. Therefore two natural questions arise for non-Hermitian systems: i) Can 2D non-Hermitian topological phases be realized using 1D lattices? 2) If so, any unique class of non-Hermitian topological phases emerges?

In this Letter we address these two important questions by showing that two unique symmetry-protected non-Hermitian topological phases can be realized in a 1D superlattice with staggered asymmetric hopping, which enable us to access to certain topological phases that otherwise are difficult to realize in Hermitian systems. Our main results are:

i) The 1D lattice hosts a 2D topological insulator phase, which is characterized by a  $2\mathbb{Z}$  Chern number in the momentum-parameter space. Such a  $2\mathbb{Z}$  Chern number is protected by a  $\mathcal{Q}$ -type-like symmetry [56], which is unique to non-Hermitian systems. Such a phase is difficult to access in Hermitian systems because it is absent in the AZ classification and requires crystalline symmetry and global  $\mathbb{Z}_2$  symmetry [58].

ii) A topological semimetal phase hosting complex Dirac points and zero modes is found to be associated with a  $\mathbb{Z}_2$  invariant, which is extracted from the normalized Berry phase for non-Hermitian systems.

iii) The system may support edge states with real energy due to a robust  $\mathcal{PT}$ -symmetric phase. In most non-Hermitian systems with on-site gain and loss, the  $\mathcal{PT}$ -symmetric phase becomes fragile with increasing system size. However, in our system, the  $\mathcal{PT}$ -symmetric phase is robust to varying chain length.

iv) There exists a mixing phase, where the zero modes and chiral surface wave coexist in proper parameter

spaces.

*v)* We discuss the experimental realization in atomic and photonic systems and propose a minimal model for achieving these phases. Our model is accessible to experiments with current technologies.

**Model Hamiltonian and symmetries.** We consider a lattice system with the nearest neighbor hopping, which can be described by the following tight-binding Hamiltonian  $H_r = \sum_i (t_{i,i+1} \hat{c}_i^\dagger \hat{c}_{i+1} + t_{i+1,i} \hat{c}_{i+1}^\dagger \hat{c}_i) + V_i \hat{c}_i^\dagger \hat{c}_i$ , where  $\hat{c}_i^\dagger (\hat{c}_i)$  is the creation (annihilation) operator of some well-defined local modes at site  $i$  and the summation with respect to  $i$  runs over all  $N_L$  lattice sites. The hopping term is non-Hermitian in the sense that  $t_{i,i+1} \neq t_{i+1,i}^*$ . For the illustration purpose, we assume a uniform on-site potential and staggered hopping terms  $t_{i,i+1} = 1 + \lambda \cos(2\pi\alpha i + \phi_L)$  and  $t_{i+1,i} = 1 - \lambda \cos(2\pi\alpha i + \phi_L)$ , where  $\lambda, \alpha \in \mathbb{R}$ . We mainly consider the cases when  $\alpha$  is rational so that it could be written as the quotient of two relative prime integers  $\alpha = p/q$ ,  $p, q \in \mathbb{Z}$ . We presume  $p, q$  are positive and  $p < [q/2]$  without loss of generality. Under the assumption of rational  $\alpha$ , the Bloch Hamiltonian reads  $e^{ik} t_{j,j+1} \psi_{j+1} + e^{-ik} t_{j,j-1} \psi_{j-1} + V_j \psi_j = \omega \psi_j$ , where the Brillouin zone ranges over  $|k| \leq \pi/q$ . To regularize the periodicity of the eigenstates in the first Brillouin Zone, we take the unitary transformations  $\psi_j \rightarrow e^{-i(q-j)k} \psi_j$  and denote the matrix Hamiltonian in the new basis as  $H(k, \phi_L)$ .

We first note that  $H^*(k, \phi_L) = H(-k, \phi_L)$  so that the real (complex) part of the  $k$ -space band is symmetric (antisymmetric) to  $k = 0$ . This also defines a time-reversal symmetry  $\mathcal{T}_k = K$ , which only reverses the sign of  $k$  and  $K$  is the operation of complex conjugate. We also have  $H(k, \phi_L) = H^T(-k, \phi_L + \pi)$ , which gives  $H(k, \phi_L) = H^\dagger(k, \phi_L + \pi)$  when combined with the time-reversal symmetry. This  $\mathcal{Q}$ -type-like symmetry protects the  $2\mathbb{Z}$  Chern insulator phase [59].

A particle-hole symmetry reversing only the sign of  $\phi_L$  is found as  $\mathcal{P}_{\phi_L} H(k, \phi_L) \mathcal{P}_{\phi_L}^{-1} = H^T(k, -\phi_L)$ , where  $\mathcal{P}_{\phi_L}$  has a permutation representation  $(q, 1)(q-1, 2)(q-2, 3) \dots$  in 2-cycle forms [60]. When combined with  $H(k, \phi_L) = H^T(-k, \phi_L + \pi)$ , this symmetry further defines an inversion (glide) symmetry along  $k$  ( $\phi_L$ ),  $\mathcal{I}_k H(k, \phi_L) \mathcal{I}_k^{-1} = H(-k, -\phi_L + \pi)$ . This yields a strong inversion symmetry  $\mathcal{I}_k H(k, \phi_L) \mathcal{I}_k^{-1} = H(-k, \phi_L)$  at high-symmetry points  $\phi_L = \frac{\pi}{2}$  and  $\phi_L = \frac{3}{2}\pi$ , which also dictate the quantization of normalized Berry phase [59]. From the particle-hole symmetry and time-reversal symmetry, we can define a  $\mathcal{Q}$ -symmetry  $\mathcal{Q} H(k, \phi_L) \mathcal{Q}^{-1} = H^\dagger(-k, -\phi_L)$ , which guarantees the quantization of Berry phase at  $\phi_L = 0$  and  $\phi_L = \pi$  [59]. When  $q$  is even, we could find a chiral symmetry  $\mathcal{C} = I_{q/2} \otimes \sigma_z$  with  $\mathcal{C}^{-1} H(k, \phi_L) \mathcal{C} = -H(k, \phi_L)$ , where  $I_n$  is a  $n$  by  $n$  identity matrix and  $\sigma_i$  is a Pauli matrix. The above symmetries are crucial for understanding the non-Hermitian topological phases [59].

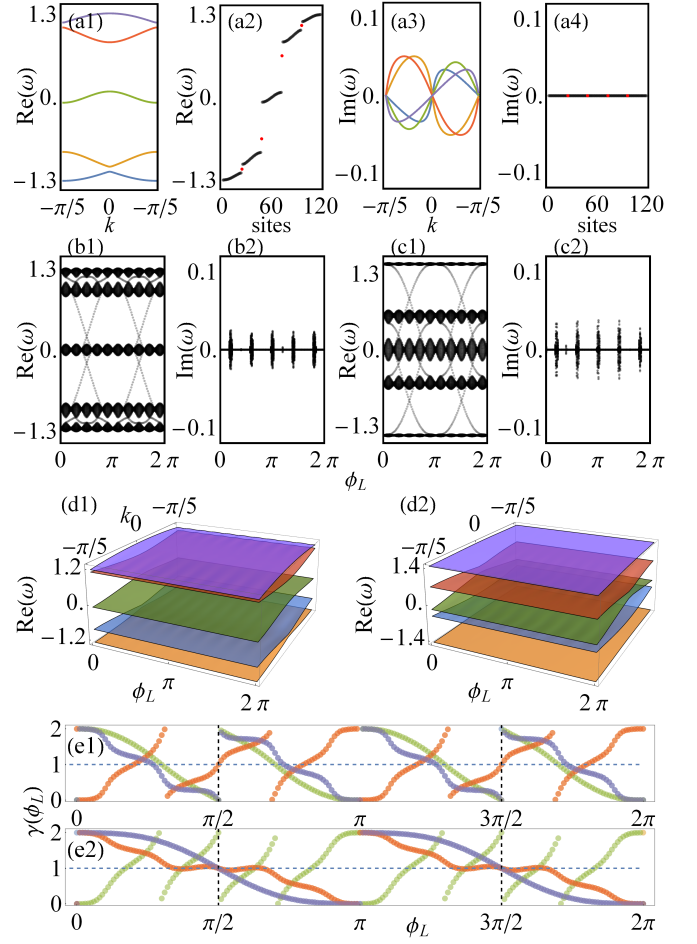


FIG. 1: (a) Bulk bands, together with energy level distributions under open boundary condition, are plotted with  $\alpha = 1/5$ ,  $\lambda = 1$ ,  $\phi_L = \pi/3$  and  $N_L = 120$ . The four edge states are highlighted with red dots. (b,c) Open-boundary spectra with varying  $\phi_L$  for  $\alpha = 1/5$  and  $\alpha = 2/5$  at  $\lambda = 1$ .  $N_L = 120$ . (d) The corresponding 2D band structure in momentum-parameter space with the same bulk parameters in (b) (panel (d1)) and (c) (panel (d2)). The Chern numbers are  $-4, 6, -4, 6, -4$  and  $-2, -2, 8, -2, -2$  from bottom to top respectively. (e) Berry curvature  $\gamma(\phi_L)$  for bulk bands in (b) (panel (e1)) and (c) (panel (e2)). The dashed vertical lines indicate inversion-symmetric points.

**$2\mathbb{Z}$  Chern insulator.** We start with the Chern insulator phase and first look at a specific example  $\alpha = 1/5$  shown in Fig. 1(a). The bulk band (Fig. 1(a1) and (a3)) has the expected symmetry  $\omega(k) = \omega(-k)^*$  and could be gapped in entire momentum space for any  $\phi_L$ . With properly chosen  $\phi_L$ , we observe two pairs of edge states labelled by red dots in Fig. 1(a2) and (a4), evolving from the bulk spectrum. Although the bulk bands could be imaginary away from the  $\mathcal{Q}$ -symmetric points in  $k$ -space, the open-boundary spectra are astonishingly real and so do the edge modes (Fig. 1(a4)).

To further explore the topological properties, we plot the open-boundary spectrum with varying  $\phi_L$  in

Fig. 1(b). Since we have  $H_O(\phi_L) = H_O(\phi_L + \pi)^T$ , the spectrum is symmetric to  $\phi_L = \pi$ , where  $H_O(\phi_L)$  denotes the open-boundary Hamiltonian. When  $N_L/q \in \mathbb{Z}$ , the bulk chiral symmetry  $\mathcal{C}$  could be generalized to  $\mathcal{C}_O = I_{N_L/q} \otimes \mathcal{C}$  so that  $\mathcal{C}_O H_O(\phi_L) \mathcal{C}_O^{-1} = H_O(\phi_L)$ . This means that the open-boundary spectrum should also be symmetric to  $\omega = 0$ . The spectra in Fig. 1(b) and (c) satisfy the above conditions with small numeric errors, which are significantly enhanced when diagonalizing a non-Hermitian Hamiltonian. The gaps persist when we tune  $\phi_L$  and there emerge four and two “chiral” surface waves propagating along  $\phi_L$  within two top gaps. A similar picture can also be seen with  $\alpha = 2/5$ , shown in Fig. 1(c). This mimics an integer quantum Hall effect in 2D if we regard  $\phi_L$  as a good quantum number under periodic boundary condition. We plot the 2D band structures in momentum-parameter space in Fig. 1(d) for  $\alpha = 1/5$  and  $\alpha = 2/5$  respectively. We find that the band topology can then be characterized by Chern number  $C^{ab} = \frac{1}{2\pi} \int dk d\phi_L (\partial_k \mathcal{A}_{\phi_L}^{ab} - \partial_{\phi_L} \mathcal{A}_k^{ab})$ ,  $a, b = L, R$ , where the Berry connections are defined as  $\mathcal{A}_k^{ab} = -i_a \langle \psi(k, \phi_L) | \partial_k \psi(k, \phi_L) \rangle_b$  and  $\mathcal{A}_{\phi_L}^{ab} = -i_a \langle \psi(k, \phi_L) | \partial_{\phi_L} \psi(k, \phi_L) \rangle_b$ . The right and left eigenstates for computing Berry connections are  $H(k, \phi_L) |\psi(k, \phi_L)\rangle_R = \omega(k, \phi_L) |\psi(k, \phi_L)\rangle_R$  and  $H(k, \phi_L)^\dagger |\psi(k, \phi_L)\rangle_L = \omega^*(k, \phi_L) |\psi(k, \phi_L)\rangle_L$  by definition. Although the four Chern numbers  $C^{ab}$  are equivalent [39], such a statement does not hold for 1D topological invariant as we will see later. We numerically compute  $C^{LR}$  here (see the caption of Fig. 1(d)).

In general, with this topological invariant, a well-defined bulk-edge correspondence could be illustrated in the complex plane. For example, the lower two bands in Fig. 1(d1) have Chern number  $C_1 = -4$  and  $C_2 = 6$ . Therefore there are 4 or 2 chiral surface waves connecting the bands in complex plane. The Chern numbers in both cases are found to be a multiple of 2. This is not a coincidence since the Chern number is doubled when integrated along  $\phi_L$  due to  $H(k, \phi_L) = H(k, \phi_L + \pi)^\dagger$ , rendering a  $2\mathbb{Z}$  Chern insulator phase [59].

The gapless edge states are also closely related to 1D topology. The edge states cross at inversion-symmetric points, especially  $\phi_L = \frac{\pi}{2}$  and  $\phi_L = \frac{3}{2}\pi$  with the strong inversion symmetry. The chiral surface waves tend to cross these two points with priority when the corresponding (normalized) Berry phase  $\gamma(\phi_L) = \frac{1}{\pi} \oint dk \mathcal{A}_k^n$  is quantized to non-trivial value  $\gamma(\phi_L) = 1$ , where the normalized Berry connection is given as  $\mathcal{A}_k^n = \frac{1}{2} (\mathcal{A}_k^{RL} + \mathcal{A}_k^{LR})$  [59]. A numeric example is given in Fig. 1(e1), verifying the quantization of Berry phases of relevant bands at high-symmetry points of both inversion and  $\mathcal{Q}$  symmetries. It also confirms the symmetry arguments because the Berry phase shows a period  $\pi$  and is anti-symmetric to  $\phi = \pi$  [59]. We would also like to remark that Fig. 1(e1) describes a charge pumping process with respect to  $\phi_L$ , so that the accumulation of Berry phase

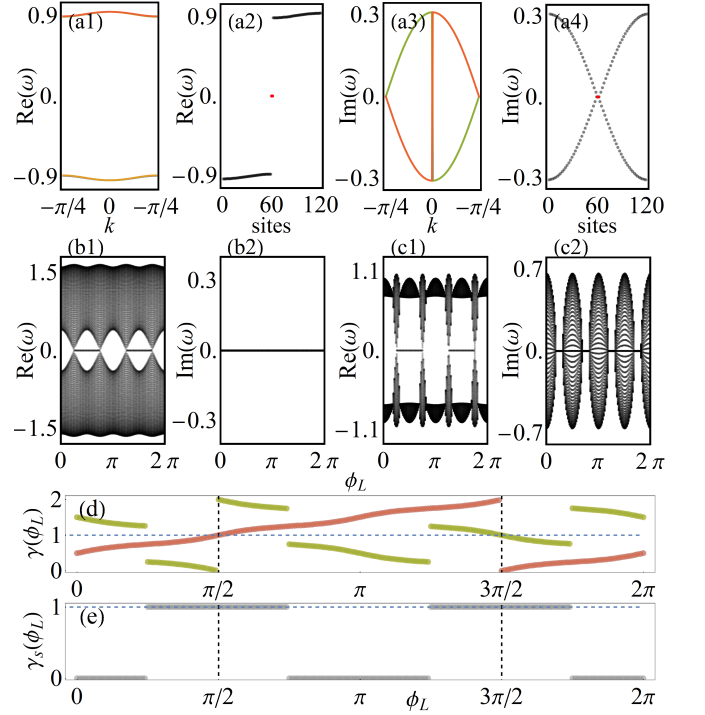


FIG. 2: (a) Bulk bands, together with energy level distributions under open boundary condition, are plotted with  $\alpha = 1/4$ ,  $\lambda = 1.1$ ,  $\phi_L = 2\pi/5$  and  $N_L = 120$ . The two-fold degenerate zero-modes are highlighted with red dots. (b,c) Open-boundary spectrums with varying  $\phi_L$  for  $\alpha = 1/4$  at (b) weak  $\lambda = 0.8$  and (c) strong  $\lambda = 1.2$ . (d) Berry phase  $\gamma(\phi_L)$  and the parameters are the same as in panel (b). The dashed vertical lines indicate inversion-symmetric points and the numeric errors are more significant near gap closing points. (e) The  $\mathbb{Z}_2$  invariant computed from panel (d).

from  $\phi_L = 0$  to  $2\pi$  gives the Chern number of each band (the normalized Berry phase also defines a Chern number  $C^n = C^{ab}$  [59]). All discussions above could be applied to  $\alpha = 2/5$  as shown in Fig. 1(e2).

We note that the summation of the Berry phase always vanishes (also holds for even  $q$ ) and this suggests that the so-called global Berry phase, which has been used to study similar 1D non-Hermitian systems [47, 61], does not apply here. The topological invariant (including Chern number and the following  $\mathbb{Z}_2$  invariant) always sums to zero as the non-Hermiticity here does not affect the additivity in *sum rule* [62]. Our results suggest that this is a well-defined 2D non-Hermitian topological insulator characterized by a  $2\mathbb{Z}$  Chern number and could be realized in a 1D lattice configuration.

**$\mathbb{Z}_2$  topological semimetal.** In Fig. 2(a), we showcase both the bulk bands and edge states for this distinct topological phase. Both the bulk and open-boundary spectra follow the symmetries we discussed for odd  $q$ , however, there is an additional symmetry respected when  $q$  is even, namely, the chiral symmetry  $\mathcal{C}$ . So the bulk bands are also symmetric to  $\omega = 0$ , which allows a finite band gap

at zero energy. Under open-boundary conditions with proper  $\phi_L$ , this gap hosts a pair of edge modes, which locate at each end of the 1D chain, as shown in Fig. 2(a2). The two-fold degenerate edge modes have exact zero and purely real energy, despite the non-Hermiticity of the system. The edge states are protected by chiral symmetry  $\mathcal{C}$  in the sense that the symmetry dictates the number of modes with  $\omega = 0$  must change by 2, so the localized state on each end is topologically protected by this symmetry.

The energy level with respect to  $\phi_L$  is given in Fig. 2(b) and (c) with weak and strong modulation strength  $\lambda$ . The spectrum is real in the former case. We observe that the edge modes persist at different  $\lambda$  in the same intervals of  $\phi_L$ . There exists gap closing points at certain inversion-symmetric points  $\phi_L$  and  $k = 0$ . Such gap closings result in a semimetal phase in momentum-parameter space and thus, the topology cannot be characterized by Chern number anymore. These gap closings represent complex Dirac points and we compute its topological charge via winding number  $w = \frac{1}{\pi} \oint_L dk d\phi_L \mathcal{A}_{k, \phi_L}^n$ , where  $L$  is a loop in momentum-parameter space encircling the complex Dirac point. The non-trivial topology of the complex Dirac points  $w = 1$  indicates topological phase transitions, which are consistent with our previous discussions on topological protection of these zero-energy modes.

The topological invariant associated with these zero modes come from the normalized Berry phase  $\gamma(\phi_L)$  and we have computed it numerically in Fig. 2(d). Only the quantization of Berry phase at inversion-symmetric points survives since it does not require a gapped bulk [59]. The two bands  $\Re(\omega) > 0$  have the same Berry phase as the two  $\Re(\omega) < 0$ . We define topological invariant  $\gamma_s(\phi_L) = \sum_j \gamma_j(\phi_L) \bmod 2$ , where the summation runs over the hole branch ( $\Re(\omega) < 0$ ). This defines a  $\mathbb{Z}_2$  invariant, where  $\gamma_s(\phi_L) = 1/0$  corresponds to topological/trivial phase. We compute this  $\mathbb{Z}_2$  invariant in Fig. 2(e) and find that it is quantized to 1 when  $\frac{1}{4}\pi < \phi_L < \frac{3}{4}\pi$ ,  $\frac{5}{4}\pi < \phi_L < \frac{7}{4}\pi$  and 0 otherwise. Thus it is congruous with the edge states and gap closing discussed in Fig. 2(a-c). Since the bulk bands could be degenerate at high-symmetric points in momentum space, we apply a chiral-symmetry-preserving perturbation  $t_{i+1,i} = 1 - \lambda \cos(2\pi\alpha i + \phi_L + \delta\phi_L)$  with infinitesimal  $\delta\phi_L$  when computing the Berry phases and  $\mathbb{Z}_2$  invariant [59]. We remark that a finite  $\delta\phi_L$  could render a  $\mathbb{Z}$ -type Chern insulator phase [59].

**Robust  $\mathcal{PT}$  symmetry and coexisting phase.** So far, we have observed that the open-boundary spectrum in this system is surprisingly real even when the bulk bands themselves are imaginary. This is remarkably different from most non-Hermitian systems and in fact, a result of the robust  $\mathcal{PT}$ -symmetric phase. The  $\mathcal{PT}$  symmetry is generally fragile in the sense that the critical value of driving term becomes very small when the system size is

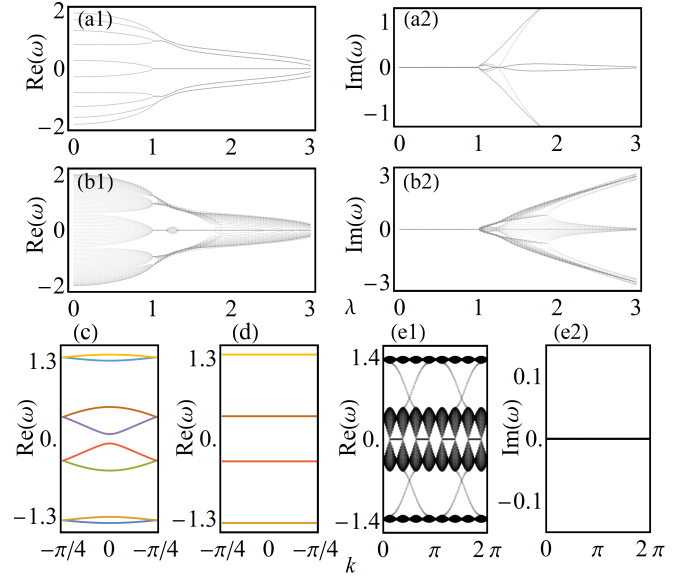


FIG. 3: (a) Open-boundary spectrum with respect to varying  $\lambda$  for  $\alpha = 1/5$ ,  $\phi_L = 0$  and  $N_L = 10$ . (b) Similar as (a) except  $N_L = 120$ . (c) Bulk bands when  $\alpha = 1/8$ ,  $\lambda = 1$  and  $\phi_L = 0.1\pi$ . (d) Flat bands at high-symmetry points  $\phi_L = \pi/4$ . Other parameters are same as panel (c). (e) Coexistence of chiral surface wave and zero modes at  $\alpha = 1/8$  and  $\lambda = 1$ .

very large [59, 63]. In contrary, the  $\mathcal{PT}$ -symmetric phase here is extremely robust and cannot be spontaneously broken when  $\lambda < 1$  regardless of the chain length  $N_L$ . As an example, we showcase the spectrum of an open chain with different length  $N_L$  in Fig. 3(a) and (b). The  $\mathcal{PT}$  symmetry is only partially broken at a fixed modulation strength  $\lambda = 1$  for both  $N_L = 10$  and  $N_L = 120$ . This notable feature of robust  $\mathcal{PT}$ -symmetric phase protects the reality of both bulk spectrum and edge modes.

As we have examined both the Chern insulator and the topological semimetal phases individually, the Chern insulator could exist for any  $q > 2$ , and the topological semimetal tends to appear when  $q$  is even since it requires chiral symmetry. This suggests that the two distinct phases could be mixed in large even  $q$ . Here, we illustrate the phase through  $\alpha = 1/8$  and a typical bulk bands are plotted in Fig. 3(c). Another feature raises here is the flat band at high-symmetry points in parameter spaces as shown in Fig. 3(d). A  $\mathcal{PT}$ -symmetric open-boundary spectrums in Fig. 3(e) manifest the coexisting phase. The topological properties can be similarly characterized with subtle due to band degeneracy [59]. Another way to mix chiral surface wave and zero mode in smaller  $q$  is tuning a finite  $\delta\phi_L$  [59].

**Discussion and conclusion.** The above model requires non-Hermitian nearest-neighbor hoppings in a lattice structure with uniform on-site potential. This could be realized in platforms like cold atoms in optical lattice or array of coupling waveguides. Many schemes have been



proposed to realize the asymmetric hopping in both lattices [53, 64]. The minimal models for realizing Chern insulator, topological semimetal and coexisting phase are  $q = 3, 2$  and  $4$  respectively [59], which remain accessible to current experiments. The chiral surface waves and zero-energy modes both have real energy in broad parameter spaces, so they are free of dissipations/amplifications over time which are easier to observe in experiments comparing to imaginary edge modes in many other models [47, 51, 63].

In addition to the two well-defined non-Hermitian topological phases, there remains much to be explored in this setup. For example, we only consider a specific configuration of many general non-Hermitian hoppings [59]. We also assume an uniform external potential and nearest neighbor hopping while staggered  $V_i$  and long-range hopping could bring richer physics as already been explored in certain bipartite superlattice [34, 37, 38].

In conclusion, we have brought up recognizable non-Hermitian 2D topological phases in a concise 1D lattice model with staggered non-Hermitian hoppings. Both the  $2\mathbb{Z}$  Chern insulator and  $\mathbb{Z}_2$  topological semimetal phases could have real-valued edge modes and are accessible in current atomic/photonic experiments. Our work explores characteristic non-Hermitian topologies in 1D and provides guidance for experimental study of non-Hermitian topological phases.

This work is supported by Air Force Office of Scientific Research (FA9550-16-1-0387), National Science Foundation (PHY-1505496, PHY-1806227), and Army Research Office (W911NF-17-1-0128). This work is also supported in part by NSFC under the grant No. 11504285 and the Scientific Research Program Funded by Natural Science Basic Research Plan in Shaanxi Province of China (Program No. 2018JQ1058),

---

\* Electronic address: [chuanwei.zhang@utdallas.edu](mailto:chuanwei.zhang@utdallas.edu)

- [1] D. Xiao, M.-C. Chang, and Q. Niu, *Berry phase effects on electronic properties*, *Rev. Mod. Phys.* **82**, 1959 (2010).
- [2] C.-K. Chiu, J. C. Y. Teo, A. P. Schnyder, and S. Ryu, *Classification of topological quantum matter with symmetries*, *Rev. Mod. Phys.* **88**, 035005 (2016).
- [3] J. Wang & S.-C. Zhang, *Topological states of condensed matter*, *Nat. Mater.* **16**, 1062 (2017).
- [4] M. Aidelsburger, M. Atala, M. Lohse, J. T. Barreiro, B. Paredes, and I. Bloch, *Realization of the Hofstadter Hamiltonian with Ultracold Atoms in Optical Lattices*, *Phys. Rev. Lett.* **111**, 185301 (2013).
- [5] M. Atala et al, *Direct measurement of the Zak phase in topological Bloch bands*, *Nat. Phys.* **9**, 795 (2013).
- [6] M. Aidelsburger et al, *Measuring the Chern number of Hofstadter bands with ultracold bosonic atoms*, *Nat. Phys.* **11**, 162 (2014).
- [7] G. Jotzu et al, *Experimental realization of the topological Haldane model with ultracold fermions*, *Nature* **515**, 237 (2014).
- [8] M. Lohse, C. Schweizer, O. Zilberberg, M. Aidelsburger, and I. Bloch, *A Thouless quantum pump with ultracold bosonic atoms in an optical superlattice*, *Nat. Phys.* **12**, 350 (2015).
- [9] S. Nakajima et al, *Topological Thouless pumping of ultracold fermions*, *Nat. Phys.* **12**, 296 (2016).
- [10] N. Goldman, J. C. Budich, and P. Zoller, *Topological quantum matter with ultracold gases in optical lattices*, *Nat. Phys.* **12**, 639 (2016).
- [11] N. R. Cooper, J. Dalibard, I. B. Spielman, *Topological Bands for Ultracold Atoms*, *Rev. Mod. Phys.* **91**, 015005 (2019).
- [12] F. D. M. Haldane and S. Raghu, *Possible Realization of Directional Optical Waveguides in Photonic Crystals with Broken Time-Reversal Symmetry*, *Phys. Rev. Lett.* **100**, 013904 (2008).
- [13] Z. Wang, Y. Chong, J. D. Joannopoulos & M. Soljacic, *Observation of unidirectional backscattering-immune topological electromagnetic states*, *Nature (London)* **491**, 772 (2009).
- [14] L. Lu et al, *Symmetry-protected topological photonic crystal in three dimensions*, *Nat. Phys.* **12**, 337 (2010).
- [15] L. Lu, J. D. Joannopoulos & M. Soljacic, *Topological photonics*, *Nat. Photonics* **8**, 821 (2014).
- [16] A. B. Khanikaev & G. Shvets, *Two-dimensional topological photonics*, *Nat. Photonics* **11**, 763 (2014).
- [17] G. Siroki, P. A. Huidobro, and V. Giannini, *Topological photonics: From crystals to particles*, *Phys. Rev. B* **96**, 041408 (2017).
- [18] B. Bahari et al, *Nonreciprocal lasing in topological cavities of arbitrary geometries*, *Science* **358**, 636 (2017).
- [19] C. He et al, *Acoustic topological insulator and robust one-way sound transport*, *Nat. Phys.* **12**, 1124 (2016).
- [20] H. He et al, *Topological negative refraction of surface acoustic waves in a Weyl phononic crystal*, *Nature* **560**, 61 (2018).
- [21] S. Imhof et al, *Topoelectrical-circuit realization of topological corner modes*, *Nat. Phys.* **14**, 925 (2018).
- [22] J.-H. Wu, M. Artoni, and G. C. La Rocca, *Non-Hermitian Degeneracies and Unidirectional Reflectionless Atomic Lattices*, *Phys. Rev. Lett.* **113**, 123004 (2014).
- [23] M. Kreibich, J. Main, H. Cartarius, and G. Wunner, *Realizing  $PT$ -symmetric non-Hermiticity with ultracold atoms and Hermitian multiwell potentials*, *Phys. Rev. A* **90**, 033630 (2014).
- [24] J. Li et al, *Observation of parity-time symmetry breaking transitions in a dissipative Floquet system of ultracold atoms*, *Nat. Commun.* **10**, 855 (2019).
- [25] F. Mostafavi, L. Yuan, and H. Ramezani, *Eigenstates Transition without Undergoing an Adiabatic Process*, *Phys. Rev. Lett.* **122**, 050404 (2019).
- [26] L. Pan, S. Chen, X. Cui, *Interacting non-Hermitian ultracold bosonic systems in three-dimensional harmonic trap: two-body exact solutions and high-order exceptional points*, *arXiv:1902.04769* (2019).
- [27] K. Yamamoto et al, *Theory of Non-Hermitian Fermionic Superfluidity with a Complex-Valued Interaction*, *arXiv:1903.04720* (2019).
- [28] K. G. Makris, R. El-Ganainy, D. N. Christodoulides, and Z. H. Musslimani, *Beam Dynamics in  $PT$  Symmetric Optical Lattices*, *Phys. Rev. Lett.* **100**, 103904 (2008).
- [29] A. Regensburger et al., *Parity-time synthetic photonic*

- lattices, *Nature* **488**, 167 (2012).
- [30] B. Peng et al., *Loss-induced suppression and revival of lasing*, *Science* **364**, 328 (2012).
  - [31] J. M. Zeuner et al, *Observation of a Topological Transition in the Bulk of a Non-Hermitian System*, *Phys. Rev. Lett.* **115**, 040402 (2015).
  - [32] L. Feng, R. El-Ganainy & L. Ge, *Non-Hermitian photonics based on parity-time symmetry*, *Nat. Photonics* **11**, 752 (2017).
  - [33] J. Hou, Z. Li, Q. Gu, C. Zhang, *Non-Hermitian Photonics based on Charge-Parity Symmetry*, [arXiv:1904.05260](#) (2019).
  - [34] T. E. Lee, *Anomalous Edge State in a Non-Hermitian Lattice*, *Phys. Rev. Lett.* **116**, 133903 (2016).
  - [35] F. K. Kunst, E. Edvardsson, J. C. Budich, and E. J. Bergholtz, *Biorthogonal Bulk-Boundary Correspondence in Non-Hermitian Systems*, *Phys. Rev. Lett.* **121**, 026808 (2018).
  - [36] S. Yao, F. Song, and Z. Wang, *Non-Hermitian Chern Bands*, *Phys. Rev. Lett.* **121**, 136802 (2018).
  - [37] S. Yao and Z. Wang, *Edge States and Topological Invariants of Non-Hermitian Systems*, *Phys. Rev. Lett.* **121**, 086803 (2018).
  - [38] S. Lieu, *Topological phases in the non-Hermitian Su-Schrieffer-Heeger model*, *Phys. Rev. B* **97**, 045106 (2018).
  - [39] H. Shen, B. Zhen, and L. Fu, *Topological Band Theory for Non-Hermitian Hamiltonians*, *Phys. Rev. Lett.* **120**, 146402 (2018).
  - [40] L. Jin and Z. Song, *Bulk-boundary correspondence in a non-Hermitian system in one dimension with chiral inversion symmetry*, *Phys. Rev. B* **99**, 081103 (2019).
  - [41] K. Kawabata, S. Higashikawa, Z. Gong, Y. Ashida, and M. Ueda, *Topological unification of time-reversal and particle-hole symmetries in non-Hermitian physics*, *Nat. Commun.* **10**, 297 (2019).
  - [42] S. Lin, L. Jin, and Z. Song, *Symmetry protected topological phases characterized by isolated exceptional points*, *Phys. Rev. B* **99**, 165148 (2019).
  - [43] S. Malzard, C. Poli, and H. Schomerus, *Topologically Protected Defect States in Open Photonic Systems with Non-Hermitian Charge-Conjugation and Parity-Time Symmetry*, *Phys. Rev. Lett.* **115**, 200402 (2015).
  - [44] P. St-Jean et al., *Lasing in topological edge states of a one-dimensional lattice*, *Nat. Photonics* **11**, 651 (2017).
  - [45] M. A. Bandres et al., *Topological insulator laser: Experiments*, *Science* **359**, 6381 (2018).
  - [46] M. Parto et al., *Edge-Mode Lasing in 1D Topological Active Arrays*, *Phys. Rev. Lett.* **120**, 113901 (2018).
  - [47] K. Takata and M. Notomi, *Photonic Topological Insulating Phase Induced Solely by Gain and Loss*, *Phys. Rev. Lett.* **121**, 213902 (2018).
  - [48] H. Zhou et al, *Observation of bulk Fermi arc and polarization half charge from paired exceptional points*, *Science* **359**, 1009 (2018).
  - [49] A. Cerjan et al, *Experimental realization of a Weyl exceptional ring*, [arXiv:1808.09541](#) (2018).
  - [50] J. Hou, Z. Li, X.-W. Luo, Q. Gu, C. Zhang, *Topological bands and triply-degenerate points in non-Hermitian hyperbolic metamaterials*, [arXiv:1808.06972](#) (2018).
  - [51] X.-W. Luo and C. Zhang, *Higher-order topological corner states induced by gain and loss*, [arXiv:1903.02448](#) (2019).
  - [52] Y. Xu, S.-T. Wang, and L.-M. Duan, *Weyl Exceptional Rings in a Three-Dimensional Dissipative Cold Atomic Gas*, *Phys. Rev. Lett.* **118**, 045701 (2017).
  - [53] T. Liu et al, *Second-Order Topological Phases in Non-Hermitian Systems*, *Phys. Rev. Lett.* **122**, 213902 (2019).
  - [54] Ch. H. Lee, L. Li, J. Gong, *Hybrid higher-order skin-topological modes in non-reciprocal systems*, [arXiv:1810.11824](#) (2018).
  - [55] Z. Gong, Y. Ashida, K. Kawabata, K. Takasan, S. Higashikawa, and M. Ueda, *Topological Phases of Non-Hermitian Systems*, *Phys. Rev. X* **8**, 031079 (2018).
  - [56] D. Bernard, A. LeClair, *A Classification of Non-Hermitian Random Matrices*, [arXiv:0110649](#) (2001).
  - [57] L.-J. Lang, X. Cai, and S. Chen, *Edge States and Topological Phases in One-Dimensional Optical Superlattices*, *Phys. Rev. Lett.* **108**, 220401 (2012).
  - [58] K. Shiozaki and M. Sato, *Topology of crystalline insulators and superconductors*, *Phys. Rev. B* **90**, 165114 (2014).
  - [59] Please refer to Supplementray Material for more information.
  - [60] We would like to remark that the particle-hole symmetry, which relates  $H(k)^T$  to  $H(-k)$  is only anti-linear when  $H(k)$  is Hermitian since  $H(k)^T = H(k)^*$ . In the context of non-Hermitian systems, the particle-hole symmetry is no longer anti-linear.
  - [61] S.-D. Liang and G.-Y. Huang, *Topological invariance and global Berry phase in non-Hermitian systems*, *Phys. Rev. A* **87**, 012118 (2012).
  - [62] Y. Hatsugai, *Explicit Gauge Fixing for Degenerate Multiplets: A Generic Setup for Topological Orders*, *J. Phys. Soc. Jpn.* **73**, 2604 (2004).
  - [63] C. Yuce,  *$\mathcal{PT}$  symmetric Aubry-Andre model*, *Phys. Lett. A* **378**, 2024 (2014).
  - [64] S. Longhi, D. Gatti & G. Della Valle, *Robust light transport in non-Hermitian photonic lattices*, *Sci. Rep.* **5**, 13376 (2015).

Supplementary Material for “Topological insulators and semimetals driven by staggered non-Hermiticity hopping”

Proof of Berry phase periodicity/quantization and  $2\mathbb{Z}$  Chern number

We have made a few statement in the main text based upon physical considerations, along with some supports from numerics. Here, we show more rigorous proofs for some of the important statements. In this subsection, we first denote the the whole momentum-parameter space using  $k = (k_x, k_y)$  for the ease of notation and generality. Then, we will go back to momentum-parameter space  $(k, \phi_L)$  to draw the conclusions in a consistent notation as in the main text for the convenience of the reader.

To start, we define the right and left eigenvectors

$$H(k)|\psi(k)\rangle_R = \omega(k)|\psi(k)\rangle_R, H(k)^\dagger|\psi(k)\rangle_L = \omega^*(k)|\psi(k)\rangle_L, \quad (1)$$

with the normalization condition  ${}_R\langle\psi(k)|\psi(k)\rangle_L = 1$ . There are four different definitions of Berry connection  $\mathcal{A}_k^{ab} = -i_a\langle\psi(k)|\partial_k\psi(k)\rangle_b$ , where  $a, b = L, R$ . A natural generalization from Hermitian systems is to take  $\mathcal{A}_k^{LR}$ , however, this is not generally correct. While  $\mathcal{A}_k^{aa}$  is always real as  ${}_a\langle\psi(k)|\partial_k\psi(k)\rangle_a$  is purely imaginary in due to normalization condition. The other two  $\mathcal{A}_k^{ab}, a \neq b$  could be any complex number as the normalization condition only shows  ${}_a\langle\psi(k)|\partial_k\psi(k)\rangle_b + {}_a\langle\partial_k\psi(k)|\psi(k)\rangle_b = 0$ . To resolve this, we use a normalized Berry phase

$$\mathcal{A}_k^n = \frac{1}{2} (\mathcal{A}_k^{RL} + \mathcal{A}_k^{LR}), \quad (2)$$

which is again purely real since

$$\begin{aligned} \mathcal{A}_k^n - \mathcal{A}_k^{n*} &= -\frac{i}{2} ({}_R\langle\psi(k)|\partial_k\psi(k)\rangle_L + {}_L\langle\psi(k)|\partial_k\psi(k)\rangle_R + {}_L\langle\partial_k\psi(k)|\psi(k)\rangle_R + {}_R\langle\partial_k\psi(k)|\psi(k)\rangle_L) \\ &= -\frac{i}{2} \partial_k ({}_R\langle\psi(k)|\psi(k)\rangle_L + {}_L\langle\psi(k)|\psi(k)\rangle_R) \\ &= 0. \end{aligned} \quad (3)$$

This enables a well-defined Berry connection for non-Hermitian systems and we now use it to define (normalized) Berry phase  $\gamma = \oint dk \mathcal{A}_k^n$ , which is real and quantized on a closed loop.

We now show that such a Berry phase  $\gamma(k_y) = \oint dk_x \mathcal{A}_{k_x}^n(k_y)$  would have a periodicity  $T$  if  $H(k_x, k_y) = H^\dagger(k_x, k_y + T)$  and if we are in the  $\mathcal{PT}$ -symmetric phase with all the bands gapped (a weaker condition is that the bands are separable in real part). Starting with the definition of left eigenvector in Equ. 1 and applying the aforementioned conditions, we have  $H(k_x, k_y)|\psi(k_x, k_y - T)\rangle_L = \omega(k_x, k_y - T)|\psi(k_x, k_y - T)\rangle_L$  so that  $\mathcal{A}_{k_x}^{RL}(k_y) = \mathcal{A}_{k_x}^{LR}(k_y - T)$  and vice versa. Now, we realize that  $\mathcal{A}_{k_x}^n(k_y) = \frac{1}{2} (\mathcal{A}_{k_x}^{RL}(k_y) + \mathcal{A}_{k_x}^{LR}(k_y)) = \frac{1}{2} (\mathcal{A}_{k_x}^{LR}(k_y - T) + \mathcal{A}_{k_x}^{RL}(k_y - T)) = \mathcal{A}_{k_x}^n(k_y - T)$ . Integrating along  $k_x$ , we find the Berry phase has a similar periodicity  $\gamma(k_y) = \gamma(k_y - T)$ . Another consequence here is that the Chern number will be the multiple of some integers due to the periodicity of Berry connection. We could also define a normalized Chern number  $C^n$  based on the normalized Berry connection so that

$$\begin{aligned} C^n &= \oint dk_x dk_y (\partial_{k_x} \mathcal{A}_{k_y}^n - \partial_{k_y} \mathcal{A}_{k_x}^n) \\ &= \frac{1}{2} \left( \oint dk_x dk_y (\partial_{k_x} \mathcal{A}_{k_y}^{RL} - \partial_{k_y} \mathcal{A}_{k_x}^{RL}) + \oint dk_x dk_y (\partial_{k_x} \mathcal{A}_{k_y}^{LR} - \partial_{k_y} \mathcal{A}_{k_x}^{LR}) \right) \\ &= \frac{1}{2} (C^{RL} + C^{LR}) = C^{LR} = C^{ab}, \end{aligned} \quad (4)$$

which means the normalized Berry connection can also be used to compute the Chern number. As  $C_T^n = \oint dk_x \int_{k_y}^{k_y+T} dk_y (\partial_{k_x} \mathcal{A}_{k_y}^n - \partial_{k_y} \mathcal{A}_{k_x}^n)$  must be quantized in a fraction of the momentum space due to the quantized charge pumping along  $k_y$  demanded by the periodicity of the Berry phase, it's easy to see  $C^n = N_y C_T^n$  belongs to a  $N_y \mathbb{Z}$  type if  $k_y$  has the period  $k_y = k_y + N_y T$ .

We also claim that the Berry phase is quantized at inversion-symmetric point, to show this, we consider the symmetry  $\mathcal{P}H(k_x, k_y)\mathcal{P}^{-1} = H(-k_x, -k_y + T)$ . Such a symmetry dictates  $H(k_x, k_y)|\mathcal{P}\psi(-k_x, -k_y + T)\rangle_R = \omega(-k_x, -k_y + T)|\mathcal{P}\psi(-k_x, -k_y + T)\rangle_R$ . When the system is gapped, we have  $\mathcal{A}_{k_x}^n(k_y) = -\mathcal{A}_{-k_x}^n(-k_y + T)$ , where the condition  $\mathcal{P}^2 = I$  is used. Then the Berry phase reads  $\gamma(k_y) = \oint dk_x \mathcal{A}_{k_x}^n(k_y) = -\oint dk_x \mathcal{A}_{-k_x}^n(-k_y + T) =$

$\oint d(-k_x) \mathcal{A}_{-k_x}^n(-k_y + T) = -\oint d(k_x) \mathcal{A}_{k_x}^n(-k_y + T) = -\gamma(-k_y + T)$ . This implies that  $\gamma(k'_y) = -\gamma(k'_y)$  if  $k'_y = k'_y - T$  (i.e., the high-symmetry point), which means it can only take the quantized value 0 or  $\pi$ .

We now go back to the specific model we discussed in the main text, where  $T = \pi$  and  $k_y = \phi_L$  has a period  $2\pi$ . This means that the Berry phase satisfy  $\gamma(\phi_L) = \gamma(\phi_L \pm \pi)$  and the Chern insulator has a Chern number  $2\mathbb{Z}$  which is protected by the symmetry  $H(k, \phi_L) = H^\dagger(k, \phi_L + \pi)$ . Another constraint on Berry phase is  $\gamma(\phi_L) = -\gamma(-\phi_L \pm \pi)$  so that it is quantized at inversion-symmetric point  $\phi_L = \pm \frac{\pi}{2}$ . Combing the two conditions together, we find further  $\gamma(\phi_L) = \gamma(\phi_L + \pi) = -\gamma(-\phi_L)$  and thus, the Berry phase is also quantized at  $\phi_L = 0$  and  $\pi$ . Note that the last relation is imposed by the  $\mathcal{Q}$  symmetry, which can be similarly proofed if the bulk band is gapped in real part.

### Lifting band degeneracies in topological semimetal

In the topological semimetal phase, there could be band degeneracies in momentum space, which would obstacle the computation of Berry phase or  $\mathbb{Z}_2$  invariant. In the following, we take an example  $\alpha = 1/4$  for illustration purpose. The Bloch Hamiltonian reads

$$H = \frac{1 + \cos(4k) + i\lambda \sin(4k) \cos(\phi_L)}{2} \sigma_x \otimes \sigma_x + \frac{1 - \cos(4k) - i\lambda \sin(4k) \cos(\phi_L)}{2} \sigma_y \otimes \sigma_y + \frac{\sin(4k) + i\lambda \cos(\phi_L)(1 - \cos(4k))}{2} \sigma_x \otimes \sigma_y + \frac{\sin(4k) - i\lambda \cos(\phi_L)(1 + \cos(4k))}{2} \sigma_y \otimes \sigma_x. \quad (5)$$

The bulk bands are then solved to be

$$E_{\pm, \pm} = \pm \sqrt{-(\lambda^2 - 2) \pm \frac{1}{4} \sqrt{-4(1 + \cos(4k))(-8 + 8\lambda^2 + \lambda^4(1 - \cos(4\phi_L)))}}, \quad (6)$$

which gives

$$E_{\pm, \pm} = \pm \sqrt{2 - \lambda^2 \pm \sqrt{\frac{1}{2}(8 - 8\lambda^2 + \lambda^4(1 - \cos(4\phi_L)))}} \quad (7)$$

at the high-symmetry point  $k = 0$ . We notice that when  $\cos(4\phi_L) = -1$ , i.e.,  $\phi_L = \frac{1}{4}\pi, \frac{3}{4}\pi, \frac{5}{4}\pi, \frac{7}{4}\pi$ , the band gap would close in momentum space with  $E_{+, -} = E_{-, +} = 0$  and  $E_{+, +} = -E_{-, -} = \sqrt{2(2 - \lambda^2)}$  when  $\lambda < \sqrt{2}$ , manifesting the topological phase transition that has been discussed in the main text. We also notice that there would always be a degenerate point in the top  $E_{+, \pm} = +\sqrt{2 - \lambda^2}$  and bottom  $E_{-, \pm} = -\sqrt{2 - \lambda^2}$  two bands at  $k = \frac{\pi}{4}$ . Such a persist degeneracy prevents us from computing the topological invariant in momentum space and it is irrelevant of the topological properties since it does not depend on  $\phi_L$ . To resolve this, we apply a perturbation term on the asymmetric hopping

$$t_{i+1, i} = 1 - \lambda \cos(2\pi\alpha i + \phi_L + \delta\phi_L), \delta\phi_L \in \mathbb{R} \quad (8)$$

which perseveres the chiral symmetry so that it would not change the associated topological invariant. Such a term would break the degeneracy at  $k = \pi/4$  but preserve the gap closings at topological phase transition points, as we would expect.

Now if we allow a finite  $\delta\phi$  to be considered, few interesting points raise here. Firstly, the topological semimetal phase can be realized in a 2-level system, i.e.,  $\alpha = 1/2$  (see Fig. 4(a)). This actually realizes some of the non-Hermitian SSH model that has been discussed in previous literatures [37, 38]. Now, the  $\mathbb{Z}_2$  index reduces to the 1D Zak phase of the ground state, which can correctly characterize the non-Hermitian SSH model with chiral symmetry.

We also note that  $\delta\phi$  would spoil the  $2\mathbb{Z}$  Chern number and thus, renders a  $\mathbb{Z}$ -type Chern insulator. Moreover, since it breaks the degeneracy within the bottom and top two bands at  $\alpha = 1/4$  respectively. There would be a gap opening, providing the possibility of supporting a non-trivial Chern-insulator phase. We demonstrate these two points in Fig. 4(b), where we do observe only one chiral surface wave (for a given prorogating direction) residing within each gap. The zero modes naturally persist but have been shifted together with the topological phase transition points. The characterization of the topological properties are similar and we will not go to any detail. We remark that the gapless chiral surface wave could be gapped out in certain parameter space and this implies interesting phenomenon if one could map this model to 2D.

Finally, we remark that there is another chiral-symmetry-preserving perturbation, namely, tuning different modulation strengthes for  $t_{i+1, i} \in \mathbb{C}$  and  $t_{i, i+1} \in \mathbb{C}$ . This would also give rise to some interesting results and provide the access to more general non-Hermitian hoppings, but it is beyond the scope of this work.



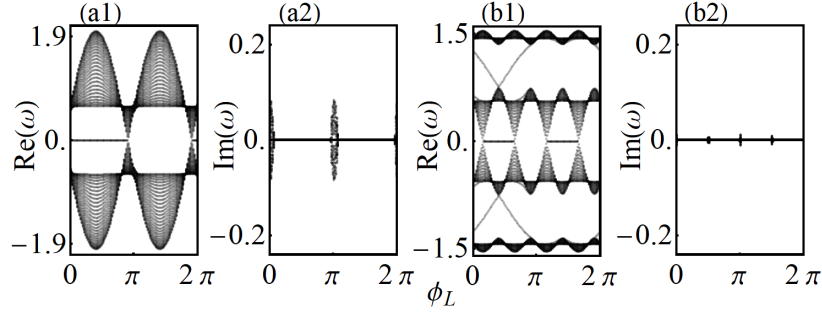


FIG. 4: (a) Open-boundary spectrum to varying  $\phi_L$  with  $\alpha = 1/2$ ,  $\lambda = 1$  and  $\delta\phi_L = 0.2\pi$ . (b) Similar as panel (a) but with  $\alpha = 1/4$ .

### Topological characterization of coexisting phase

While we have studied the two topological phases individually, the coexisting phase can be characterized in a similar way, but we need to be careful with the band degeneracies. We again apply a small perturbation  $\delta\phi_L$  when computing the Berry phase and these results are shown in Fig. 5(a). Due to the gapless phase, the Berry phase does not have the periodicity any more, however, it is still quantized at inversion-symmetric point as a small  $\delta\phi_L$  only perturb the system slightly away from strong-inversion-symmetric. As we observe in Fig. 3(e) that the chiral surface wave again crosses at these high-symmetry points.

We notice that the Chern number is not well-defined due to the topological phase transition point and degeneracies between top/bottom four bands. While the  $\delta\phi_L$  term allows us to compute the Chern number, it breaks the  $2\mathbb{Z}$  constraint. The Chern number is found to be odd for the top/bottom two bands after they are broken (see also the charge pumping in Fig. 5(a)). Now, if we gradually tune  $\delta\phi_L$  to 0, the band Chern number should not change as there is no topological phase transition happening. When  $\delta\phi_L = 0$ , they become degenerate and if we consider both as a single band, the Chern number is again even so that the chiral surface wave appear in a pair in each gap.

In comparison, the zero modes can be directly characterized by the  $\mathbb{Z}_2$  invariant. It is shown in Fig. 5(b) and is consistent with the zero modes observed in Fig. 3(e).

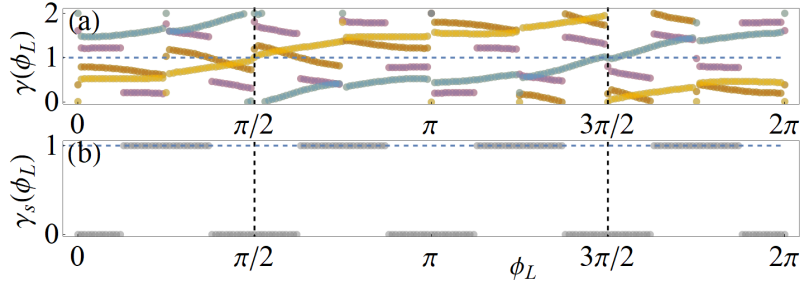


FIG. 5: (a) Berry phase  $\gamma(\phi_L)$  for the coexisting phase shown in Fig. 2(e). The dashed vertical lines indicate inversion-symmetric points and the numeric errors are more significant near gap closing points. (b) The  $\mathbb{Z}_2$  invariant computed from panel (a).

### Minimal model for Chern insulator phase

While in the main text, we illustrate the Chern insulator phase with  $q = 5$  for the purpose of comparing different gap opening schemes by tuning  $p$ , the Chern insulator can be realized with  $\alpha = 1/3$  for the ease of experimental realizations.

A typical band structure in momentum space is plotted in Fig. 6(a1) and (a3). Finite gaps are opened in the momentum-parameter space and there is a pair of edge state at certain  $\phi_L$  as shown in Fig. 6(a2). The two edge states have opposite real energy but the same density profile as plotted in Fig. 6(a4). The total spectrum to varying  $\phi_L$  in Fig. 6(b) indicate the  $2\mathbb{Z}$  Chern insulator phase. Since the  $2\mathbb{Z}$  Chern number is protected by the symmetry

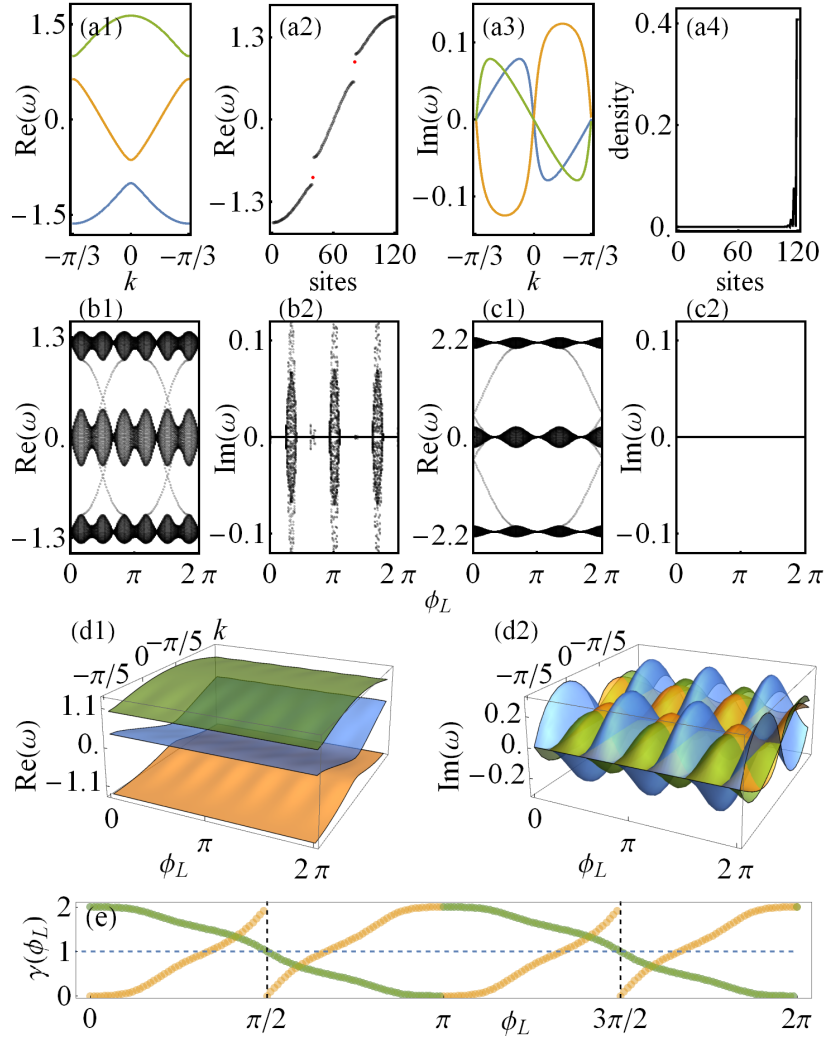


FIG. 6: (a1-a3) Bulk spectrums, together with energy level distributions under open boundary condition, are plotted with  $\alpha = 1/5$ ,  $\lambda = 1$ ,  $\phi_L = \pi/3$  and  $N_L = 120$ . The two edge states are highlighted with red dots. (a4) The density distribution of the edge state in real space. (b) Open-boundary spectrums with varying  $\phi_L$  for  $\alpha = 1/5$  and  $\lambda = 1$ . We also set  $N_L = 120$ . (c) Similar as (b) but with  $\delta\phi_L = \pi$  so that this is a  $\mathbb{Z}$  Chern insulator with odd Chern number. (d) The corresponding 2D band structure in momentum-parameter space with the same bulk parameters in (b). (e) Berry curvature  $\gamma(\phi_L)$  for bulk bands in (b). The dashed vertical lines indicate inversion-symmetric points.

$H(k, \phi_L) = H^\dagger(k, \phi_L + \pi)$  and it is broken by  $\delta\phi_L$ , the  $2\mathbb{Z}$ -type Chern insulator would become a  $\mathbb{Z}$ -type with proper  $\delta\phi_L$ . This is again illustrated in Fig. 6(c). Note that, the  $\delta\phi_L$  term also changes the  $\mathcal{PT}$ -breaking point so that the spectrums become purely real from panel (b) to (c). The topological characterization is exactly the same as discussed in main text. We show the complex bands and Berry phase  $\gamma(\phi_L)$  in Fig. 6(d) and (e), which are consonant with panel (b).

#### $\mathcal{PT}$ -symmetric phase by gain/loss is fragile

As we have discussed in main text that the usual  $\mathcal{PT}$ -symmetric phase by gain/loss is fragile so that the total spectrum cannot be purely real in the separable regime [63]. To illustrate the fragile  $\mathcal{PT}$ -symmetric phase, we consider the simplest model described by the following tight-binding Hamiltonian

$$H_{PT} = t \sum_i \left( \hat{c}_i^\dagger \hat{c}_{i+1} + h.c \right) + (-1)^i \gamma \hat{c}_i^\dagger \hat{c}_i, \quad (9)$$

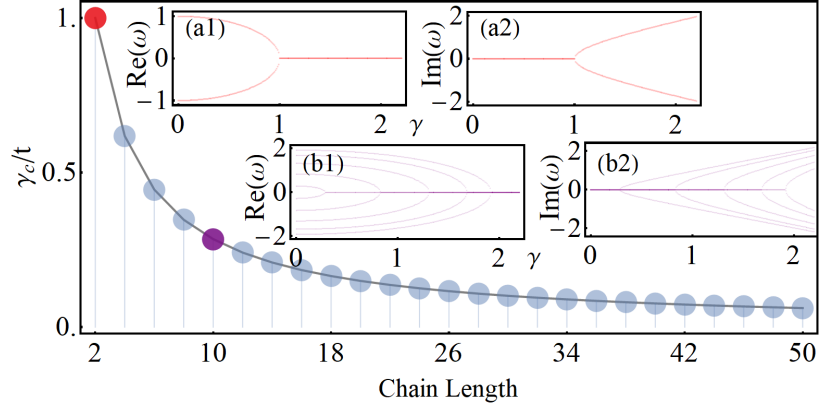


FIG. 7: Critical gain/loss rate for  $\mathcal{PT}$  breaking versus the length of the total chain in real space. The insets show how the spectrum changes to varying  $\gamma$ .

where  $\gamma > 0$  is on-site gain/loss rate. The Hamiltonian would be defective at exceptional point so that the system enters partially broken regime (part of the spectrum becomes complex) at the smallest  $\gamma_c$  satisfying  $\text{Det}(H_{PT}(\gamma_c)) = 0$ . The determinant can be solved through the recursive equation  $D_n = (-1)^n \gamma D_{n-1} - t^2 D_{n-2}$  with boundary conditions  $D_1 = -i\gamma$  and  $D_2 = \gamma^2 - t^2$ . The critical value  $\gamma_c$  is then solved for different chain length in Fig. 7, where we see a fast drop of  $\gamma_c$  when the chain length starts to increase and ultimately approaches zero. In the insets (a) and (b), we also show the spectrum to varying  $\gamma$  at different chain length 2 and 10 respectively. Such an argument could also be applied to more general cases like larger unit cell or quasiperiodic potential or even higher dimensions. This explains the complex edge states observed in many models with on-site gain and loss [47, 63].

Such a fragility does not happen when the non-Hermiticity is introduced by asymmetric hopping as illustrated in Fig. 3(a) and (b) so that our model enjoys real edge modes and thus, more accessible to experimental observations.